
Surface visco-elastic modes in a spread film of a block copolymer

Andrew S. Brown,^a Randal W. Richards,^{*a} D. Martin A. Buzza^b and Tom C. B. McLeish^b

^a *Interdisciplinary Research Centre in Polymer Science and Technology, University of Durham, Durham, UK DH1 3LE*

^b *Interdisciplinary Research Centre in Polymer Science and Technology, University of Leeds, Leeds, UK LS2 9JT*

Received 20th November 1998

A linear diblock copolymer of polymethyl methacrylate and poly-4-vinyl pyridine quaternised with ethyl bromide has been spread as a thin film at the air/water interface and the properties of the capillary waves obtained using surface quasi-elastic light scattering. The data have been analysed for surface visco-elastic parameters on the basis of the complete absence of any transverse shear viscosity in the spread film. A resonance between capillary and dilatational modes was observed at a block copolymer surface concentration of 0.8 mg m^{-2} . At this surface concentration the frequency dependence of the surface tension, dilatational modulus and dilatational viscosity exhibited behaviour which suggested that spread film could be represented as a Maxwell fluid with a relaxation time of *ca.* $3 \mu\text{s}$. This Maxwell fluid model also described the dependence of an 'apparent' relaxation time of the dilatational mode on the surface concentration for a capillary wave of fixed wavenumber. A comparison of the observed dispersion behaviour (damping as a function of capillary wave frequency) with that predicted by theoretical forms of the dispersion equation, showed that there was no need to include a postulated coupling factor. This observation concurred with the modest dimensions of the surface region occupied by the quaternised vinyl pyridine blocks.

Introduction

The presence of a polymer layer at a fluid interface imparts visco-elastic properties to the interface in addition to lowering the surface tension. Since the fluid interface is perturbed by random thermal fluctuations known as capillary waves, these visco-elastic properties resist the periodic expansion and compression of the surface layer by these waves. Capillary waves are due to the transverse motion of the surface but over 30 years ago Lucassen¹ pointed out the existence of a second surface wave associated with longitudinal, *i.e.*, in plane, motion. The existence of both accounts for the experimentally observed fact that the capillary wave damping of the surface of surfactant solutions has a maximum value rather than continuously increasing with concentration as predicted by Levich.² The two surface waves can be approximated as orthogonally coupled lossy oscillators^{3,4} and may thus be susceptible to analysis using models developed for bulk visco-elastic properties.⁵

Each surface mode has an associated modulus; for the transverse mode this modulus is the surface tension whereas the longitudinal mode has a dilatational modulus. Each of these moduli is complex, *i.e.*, they are composed of a real term, the modulus, and a frequency dependent imaginary term, which includes the transverse shear viscosity or the dilatational viscosity depending on

the mode being considered.⁶ The dilatational modulus can be significantly larger than the surface tension and hence plays an important part in damping surface waves.

An extensive analysis of surface modes in surfactant solutions was produced by Lucassen-Reynders and Lucassen⁷ based on the hydrodynamics of the surface layer and the balancing of viscous stresses by the force per unit area. The dispersion equation obtained (connecting surface wavenumber and wave frequency) has been the basis of most analyses of experimental data, together with various extensions attempting to account for such facets as bulk diffusion and possible adsorption barriers at the air/liquid interface^{8–10} of the surfactant solution. Some of these extensions were prompted by the observation of *negative* dilatational viscosity in some surfactant solutions¹¹ and in some cases these could be rationalised by citing non-equilibrium adsorption processes.

The modification of surface waves by polymers has also been considered from the theoretical viewpoint and in the main the polymers have been in solution or as gels. Harden and Pleiner¹² incorporated a transient modulus and relaxation time normal to the surface arising from polymer entanglements. The essential form of the dispersion relation was identical to that of Lucassen-Reynders and Lucassen. In common with the earlier descriptions, there was no attempt made to associate the transverse and dilatational parameters with molecular scale features of the surface polymer layer. This aspect is important because Goodrich,^{6,13} who first defined the various surface moduli, merely cites the two viscosity terms of relevance here as excess surface properties. The physical understanding of these terms becomes pressing when negative values are observed for spread polymers at the air/water interface,¹⁴ which cannot be explained by appealing to the models used for surfactants because the polymers were insoluble.

The earlier observation of negative dilatational viscosities for an amphiphilic graft copolymer prompted a re-examination of the problem from a different viewpoint adopting the features of a polymer at an interface from the outset. In parallel with this development of theory, experimental attempts were made to ascertain whether these negative dilatational viscosities were attributable to interactions between spread polymer and water subphase using a copolymer with a poly-electrolyte constituent, which has strong interactions with the aqueous subphase. We report here the results of these experiments, which are preceded by an outline of the theoretical basis for the analysis and measurement of capillary waves.

Theoretical background

We outline here the basis of surface light scattering, which enables the determination of surface visco-elastic parameters, and we give the additional features introduced by a re-analysis of the problem and which pertain specifically to polymers,¹⁵ in principle.

Surface light scattering

The thermal fluctuations perturbing a fluid surface can be decomposed into a set of discrete Fourier modes whose root mean square amplitude is *ca.* 3 Å with wavelengths of the order of 3–500 μm, as typically observed by light scattering. These waves scatter light efficiently and this scattering was first analysed for pure liquid surfaces over 30 years ago¹⁶ and has since been applied to other systems, particularly surfactant solutions and dispersions.^{14,17–27} The dispersion relation, $D(\omega)$, provides the connection between a capillary wave of wavenumber q ($=2\pi/\lambda$, where λ is the wavelength), the propagation frequency, ω , and the moduli of the surface film as well as the bulk physical parameters of the fluid. The propagation frequency is a complex quantity whose real term is the wave frequency (ω_o) and the imaginary term is the damping of the wave (Γ).

$$\omega = \omega_o + i\Gamma \quad (1)$$

The surface film moduli, in the classical capillary wave theory, are also complex terms; they are the surface tension, γ , and dilatational modulus, ϵ , expanded as linear response functions to incorporate any additional energy dissipation as viscosity terms

$$\gamma = \gamma_o + i\omega_o \gamma' \quad (2)$$

$$\epsilon = \epsilon_o + i\omega_o \epsilon' \quad (3)$$

where the subscript o indicates the elastic term and the prime its associated viscosity term.

At the air/liquid interface the dispersion equation for the capillary waves is

$$D(\omega) = [\eta\omega(q - m)]^2 + [\varepsilon q^2 + i\eta\omega(q + m)] \times [\gamma q^2 + i\eta\omega(q + m) - \rho\omega^2/q] = 0 \quad (4)$$

where ρ is the fluid density of viscosity η and $m = (q^2 + i\omega\rho/\eta)^{1/2}$. The power spectrum of the scattered light is

$$P(\omega) = -\frac{k_B T}{\pi\omega} \text{Im} \left[\frac{i\omega\eta(q + m) + \varepsilon q^2}{D(\omega)} \right] \quad (5)$$

and thus by observation of this power spectrum (or its temporal equivalent, the correlation function), the contributory factors to the dispersion may be obtained. At the air/liquid interface a coupling exists between transverse and dilatational modes that enables dilatational moduli to be evaluated from an analysis of the light scattered by the transverse (capillary) modes.

The observation of negative dilatational viscosities in solutions where a surface excess layer is formed has been rationalised by resistance to diffusional exchange.^{7,28} Such negative dilatational viscosities have also been noted in systems where an amphiphilic polymer has been spread at the air/water interface^{14,21,23} and since, in some cases, the polymer was insoluble in water, the ideas of diffusional resistance are clearly inapplicable. [The insolubility notwithstanding it was evident from neutron reflectivity that the water subphase was penetrated to a finite extent by the hydrophilic part of the copolymer.²⁹] These observations prompted a re-examination of the dispersion equation for these systems.¹⁵

Diblock copolymers at a liquid/liquid interface

The model adopted is a linear diblock copolymer located at the interface between two immiscible fluids that individually act as a solvent for a single block. As a result the block copolymer forms a brush like layer on each side of the interface, *i.e.*, a double-sided brush is formed. This layer is perturbed by a capillary wave (see Fig. 1) and this perturbation is described by the curvature of the surface and a modified Alexander–de Gennes model³⁰ describes the Helmholtz free energy of the brush. The perturbation in the Helmholtz free energy due to the capillary wave results in four parameters contributing to the Helmholtz free energy difference between the curved surface and the planar ‘equilibrium’ surface. Three of these pertain to the changes in effective surface concentration on perturbing the surface. Of these three two are already well established, the surface pressure and the dilatational modulus; the third, λ , is new and is directly related to the asymmetry of the polymer brush layer. It is termed the coupling constant because it expresses the coupling of the interfacial boundary to the concentration variation of the brushes. The fourth term, the bending modulus, κ , has no connection with the capillary wave induced change of surface concentration. Viscous dissipation of energy arises from solvent flow through the brush layers, the flow being due to volume changes of these layers as the interface where they are connected is deformed. Consequently coupling and bending modulus are complex terms

$$\lambda = \lambda_o + i\omega_o \lambda' \quad (6)$$

$$\kappa = \kappa_o + i\omega_o \kappa' \quad (7)$$

the primed terms again being the associated viscosity parameters.

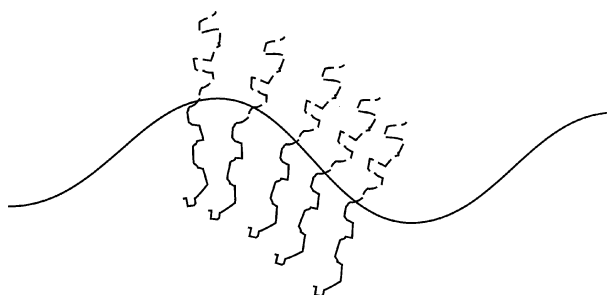


Fig. 1 Schematic diagram of double sided brush layer perturbed by capillary wave.

The bending modulus has been introduced earlier in studies of low molecular weight surfactants;^{31,32} however, it only becomes important when the surface tension is ultra low, *i.e.*, approaching zero, which is not the case here and consequently we give no more attention to it. For the interpretation of surface quasi-elastic light scattering (SQELS) data, an important factor is that a transverse shear viscosity term, γ' , does not appear; moreover this fact should apply for *all* interfacial systems not just the double sided brush layer model used. For a polymer at the air/water surface the visco-elastic parameters can be obtained by setting the molecular weight of the B block to zero. There are small differences in these parameters when they are derived by mean field or scaling theory, but the general forms are essentially the same. We quote the simpler scaling relations here for the surface pressure, π , dilatational modulus, ϵ_o , and its viscosity component, ϵ' , together with the relations for the two contributions to the coupling parameter, λ . In eqns. (8)–(10), N_A is the degree of polymerisation of the A block immersed in the subphase (of viscosity η_1), which has a grafting density (\propto surface concentration) of σ_o and a statistical step length of b . Note that because of the way in which the curvature is defined both λ and λ' are negative quantities.

$$\pi \approx \sigma_o^{11/6} b^{5/3} N_A k_B T \approx \epsilon_o \quad (8)$$

$$\lambda_o \approx \sigma_o^{13/6} b^{10/3} N_b^2 k_B T \quad (9)$$

$$\epsilon' \approx \sigma_o^2 b^5 (\eta_1 N_A^3) \quad (10)$$

$$\lambda' \approx \sigma_o^{7/3} b^{20/3} \eta_1 N_A^4 \quad (11)$$

The contribution of the coupling term, λ , to the dispersion of the capillary waves relative to that of the dilatational terms is determined by the product of the capillary wavenumber and the brush height, qh_o . From the equations above we can estimate magnitudes of each parameter using typical values for b , N_A and σ_o ; the calculated values of π , ϵ_o and ϵ' are of the correct order of magnitude; whereas λ_o and λ' are *ca.* 4–5 orders of magnitude smaller than the values of ϵ_o and ϵ' . For the contribution of λ to be significant then, qh_o should be at least 0.1; for the q values used here ($\sim 200 \text{ cm}^{-1}$) this intimates that h_o should be *ca.* $5 \mu\text{m}$! For this brush like model the dispersion equation is modified to

$$D(\omega) = [\eta\omega(q - m) + i\lambda q^3]^2 + [\epsilon q^2 + i\eta\omega(q + m)] \times [\gamma q^2 + i\eta\omega(q + m) - \rho\omega^2/q] = 0 \quad (12)$$

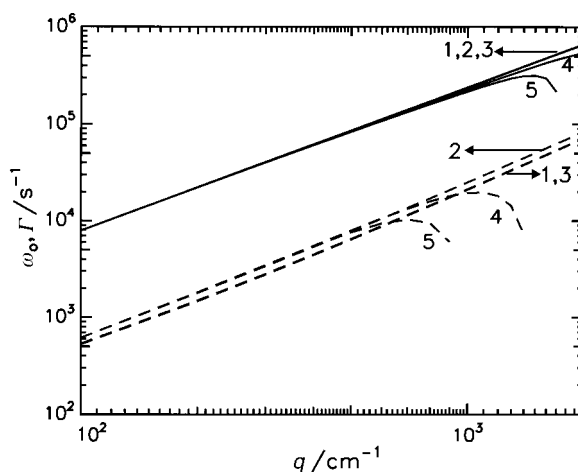
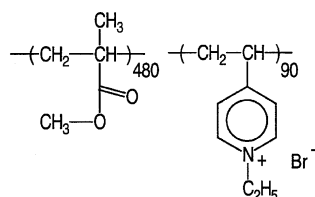


Fig. 2 Frequency (solid line) and damping (dashed lines) calculated for values of λ_o and λ' for a surface concentration of 1 mg m^{-2} of a brush like polymer layer. The values of λ_o and λ' , respectively are: curve 1, 0 and 0; curve 2, 10^{-4} and 0; curve 3, 10^{-5} and 0; curve 4, 10^{-4} and 10^{-9} ; and curve 5, 10^{-4} and 2×10^{-9} . The units of λ_o and λ' are mN m^{-1} and mN s m^{-1} .

Hence although λ_0 and λ' are considerably smaller than ε_0 and ε' , the multiplication by q^3 increases the significance of λ in the dispersion equation. Solving the dispersion equation enables us to determine the effects that λ_0 and λ' will have on the observed frequency and damping of the capillary waves. For typical values of γ_0 , ε_0 and ε' (60 mN m^{-1} , 10 mN m^{-1} and $10^{-4} \text{ mN s m}^{-1}$ respectively), keeping γ' at zero, the dependences of the capillary wave frequency and damping on λ_0 and λ' are shown in Fig. 2. The real part of the coupling parameter has little effect on the frequency in the range of q generally accessible. Additional damping is introduced by the imaginary part and eventually the capillary mode becomes over-damped and both frequency and damping fall. It appears that data at high wave numbers are necessary to be able to distinguish whether the coupling term, λ , makes a contribution.

Experimental

The amphiphilic copolymer was a linear diblock copolymer of polymethyl methacrylate and poly-4-vinyl pyridine quaternised with ethyl bromide (PMMA-VPQ). The copolymer had a methyl methacrylate mole fraction of 0.81 and the degree of polymerisation of the PMMA and quaternised 4-vinyl pyridine blocks were 480 and 90, respectively. The schematic structure of the block copolymer is shown below.



Spread films of this copolymer were obtained by depositing small volumes of approximately 0.1% w/v chloroform/methanol solutions of the copolymer on to the surface of specially purified water (at 294 K) in a rectangular Langmuir trough, this trough being in the optical path of the surface light scattering instrument. The instrument has been fully described elsewhere³³ and the

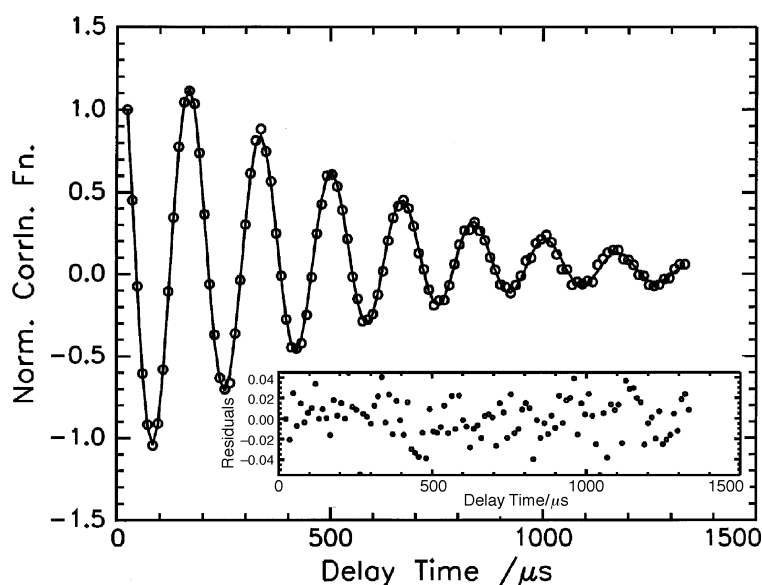


Fig. 3 Heterodyne correlation function for PMMA-VPQ block copolymer spread film, surface concentration 0.2 mg m^{-2} . The line is a fit to the data using the direct data analysis fitting method. The inset shows the residuals between fit and data.

only modification from these earlier descriptions was the use of a solid state laser producing light of wavelength 532 nm. A typical heterodyne correlation function is shown in Fig. 3 together with a fit and the residuals of the fitting process. Surface light scattering data were collected as a function of surface concentration at a fixed wavenumber, q , of 270 cm^{-1} for the capillary waves and for a fixed surface concentration, Γ_s , of 0.8 mg m^{-2} as a function of capillary wave wavenumber. The data were analysed in two ways: first, the frequency and damping were obtained by fitting a cosine function (incorporating the instrumental effects and the non-Lorentzian characteristics of the power spectrum) to the data; second, the surface visco-elastic parameters (γ_o , ε_o and ε') were obtained by the direct data analysis method pioneered by Earnshaw *et al.*³⁴

Results

Fig. 4 shows the surface pressure and Gibbs elasticity of spread films of the PMMA–VPQ copolymer spread on pure water obtained by continuously recording the surface pressure as the spread film was compressed at $30 \text{ cm}^2 \text{ min}^{-1}$ in a Langmuir trough. The initial area of the trough was $\sim 900 \text{ cm}^2$. Gibbs elasticity data were obtained using $\varepsilon_{st} = \Gamma_s(d\pi/d\Gamma_s)$ and $(d\pi/d\Gamma_s)$ was obtained by fitting an empirical polynomial to the surface pressure data and subsequent numerical differentiation. The Gibbs elasticity or dilatational modulus so obtained increases rapidly to high values over a surface concentration range between 1.1 and 1.3 mg m^{-2} ; this is followed by further increase at a less rapid rate to a maximum static dilatational modulus of $\sim 70 \text{ mN m}^{-1}$ at a surface concentration of 2.2 mg m^{-2} . At higher surface concentrations the Gibbs elasticity rapidly falls to zero. The surface pressure is essentially zero (within the accuracy of our surface balance) for surface concentrations less than 1.2 mg m^{-2} . A plateau value of $\sim 35 \text{ mN m}^{-1}$ is observed, which is a typical value for homoPMMA. However, the rise to this plateau surface pressure is much less abrupt than for PMMA homopolymer because of the VPQ block.

The nature of the spread film on the water surface is relevant to the interpretation of the surface light scattering data, *i.e.*, is the film coherent over the whole area or does the coverage become ‘patchy’ at low concentrations? To establish the nature of the spread film, surface light scattering data were repeatedly collected over a 10 h period. The variation of the frequency over this period is shown in Fig. 5; clearly there is negligible variation. Patchy coverage reveals itself as fluctuations in the frequency between the high value for pure water and the lower value for regions of the surface covered by polymer as these regions drift in and out of the laser beam incident on the surface.

The fundamental observations of surface light scattering, *i.e.*, the frequency and damping of the capillary waves, are shown in Fig. 6 as a function of the surface concentration of PMMA–VPQ.

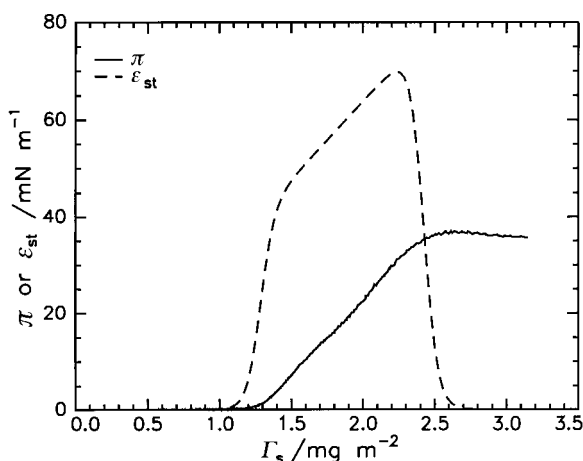


Fig. 4 Surface pressure (—) and Gibbs elasticity (---) of PMMA–VPQ spread films obtained from Wilhelmy plate measurement.

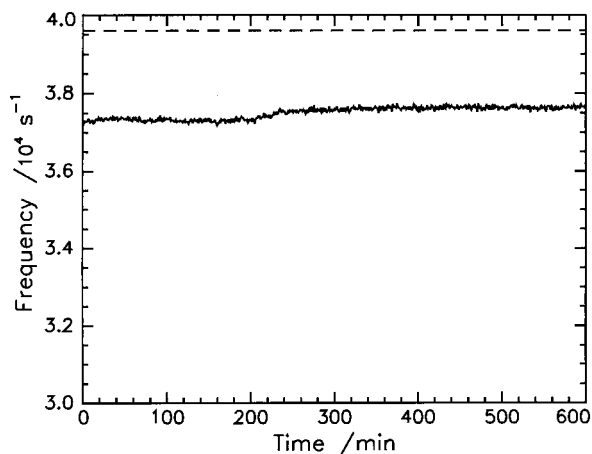


Fig. 5 Variation of capillary wave frequency with time after spreading for a spread block copolymer film at a surface concentration of 0.5 mg m^{-2} . The dashed line is the frequency of capillary waves on clean water obtained by surface quasi-elastic light scattering at the same wavenumber.

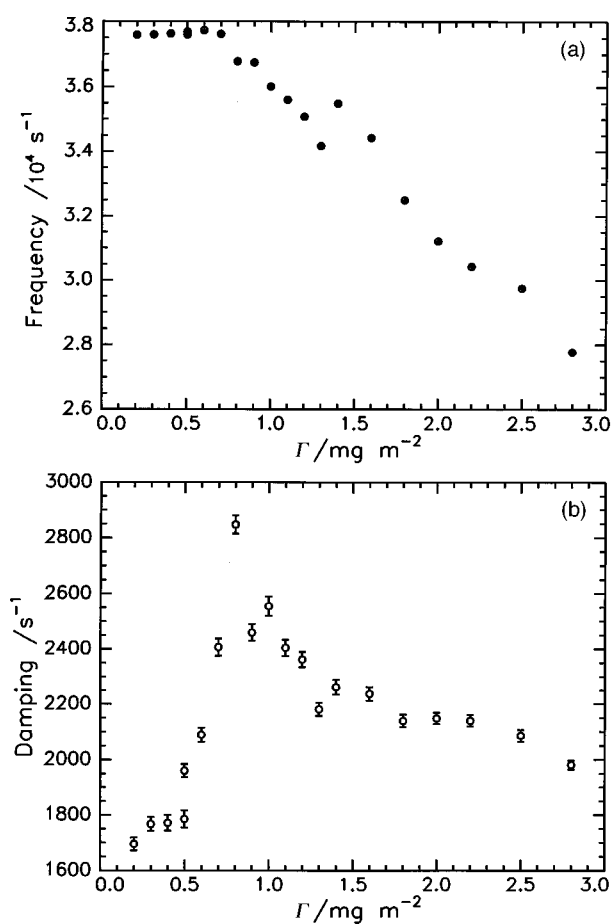


Fig. 6 Frequency (a) and damping (b) of capillary waves as a function of surface concentration of PMMA-VPQ copolymer.

The frequency has no variation up to a surface concentration of $\sim 0.7 \text{ mg m}^{-2}$, where it begins to fall. The decrease in capillary wave frequency is not monotonic, a small divergence and maximum being evident at $\Gamma_s \approx 1.3 \text{ mg m}^{-2}$. Capillary wave damping increases from the outset and has a maximum value (approaching twice that of the clean water at $\Gamma_s \approx 0.8 \text{ mg m}^{-2}$ surface) before decreasing at higher surface concentrations.

The maximum in the damping is a symptom of resonance between the transverse and longitudinal modes of the surface waves, *i.e.*, where the real frequencies of the two modes are equal. The frequencies of the capillary and dilatational modes are

$$\omega_c \approx \left(\frac{\gamma q^3}{\rho} \right)^{1/2} + \frac{i 2 \eta q^2}{\rho} \quad (13)$$

$$\omega_D \approx \frac{\sqrt{3}}{2} \left(\frac{\varepsilon^2 q^4}{\eta \rho} \right)^{1/3} + \frac{i}{2} \left(\frac{\varepsilon^2 q^4}{\eta \rho} \right)^{1/3} \quad (14)$$

and classically the resonance occurs when $\varepsilon_0/\gamma_0 \approx 0.16$. It is at this resonance where we have the maximum sensitivity to obtaining ε from surface light scattering data because the coupling between the modes is at a maximum.

Extraction of the surface visco-elastic parameters is dependent on the form of the dispersion equation used. From the re-examination of the surface modes by Buzza *et al.*¹⁵ it appears that the transverse shear viscosity is non-existent and therefore we have set γ' to zero. The bending modulus contribution will be negligible for the surface tensions observed here. Likewise the incorporation of the coupling term, λ , is dependent on the value of qh_0 . Separate neutron reflectometry experiments on spread films of this copolymer (see below) demonstrate that $qh_0 \approx 10^{-4}$ and thus the contribution of the coupling term is negligible. A typical fit to the experimental surface light scattering data is shown in Fig. 3; from such fits we obtain surface tension, dilatational modulus and dilatational viscosity.

The surface tension (Fig. 7) obtained by light scattering shows some similarities with that obtained from surface pressure data (zero frequency data), but clearly exhibits differences at higher concentrations, with the light scattering values crossing the zero frequency values. No comparison can be made between the zero frequency Gibbs elasticities and the dilatational moduli obtained from light scattering. Fig. 8 shows the behaviour is completely different. A maximum in ε_0 at $\Gamma_s \approx 1.0 \text{ mg m}^{-2}$ is noted and the light scattering values of ε_0 are an order of magnitude smaller than those extracted from the surface pressure data. This difference in dilatational modulus values has been observed in other systems.³⁵ The dilatational viscosity also exhibits a small maximum at

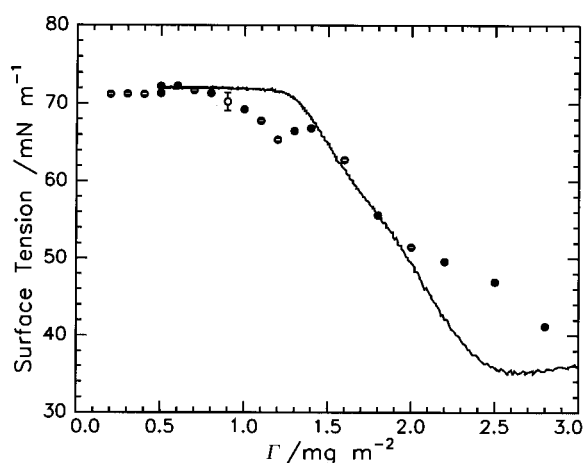


Fig. 7 Surface tension as a function of surface concentration of PMMA-VPQ obtained from SQELS data (○, partially obscured by error bars) and from the surface pressure isotherm (—).

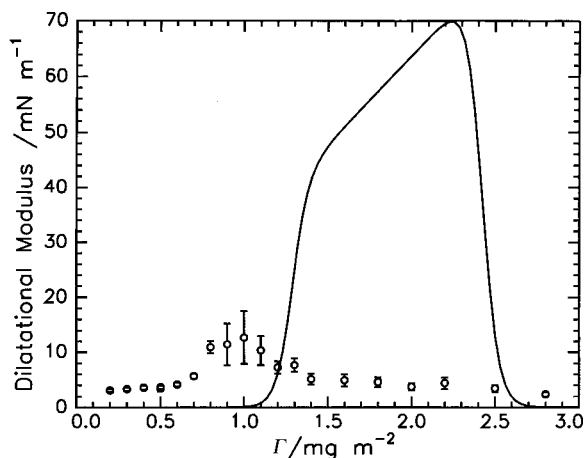


Fig. 8 Dilatational modulus as a function of block copolymer surface concentration. SQELS data (○) and surface pressure data (—).

$\Gamma_s \approx 1.3 \text{ mg m}^{-2}$, Fig. 9, where the small deviation in the decrease of capillary wave frequencies was observed.

Discussion

Surface concentration dependence

The damping maximum at a surface concentration of $\sim 0.8 \text{ mg m}^{-2}$ is commensurate with the ratio of surface tension to dilatational modulus values obtained from surface light scattering data which has a value ~ 0.16 , *i.e.*, the classical resonance position. Surface tension and dilatational modulus obtained from light scattering exhibit very different dependences on surface concentration compared to the equivalent parameters obtained from the surface pressure isotherm. The grafting density, σ_o , in eqns. (8)–(11) is directly proportional to Γ_s ; consequently we anticipate that γ_o , ε_o and ε' at a fixed q should scale with Γ_s , as given in the previously cited equations. There is partial agreement with these predictions in that ε_o scales with Γ_s with an exponent of ~ 2.2 for Γ_s between 0.5 and 1.0 mg m^{-2} and ε' has an exponent of ~ 2 for all values of Γ_s up to $\Gamma_s = 1.0 \text{ mg m}^{-2}$. However there are also disagreements. First, the surface pressure derived from surface light

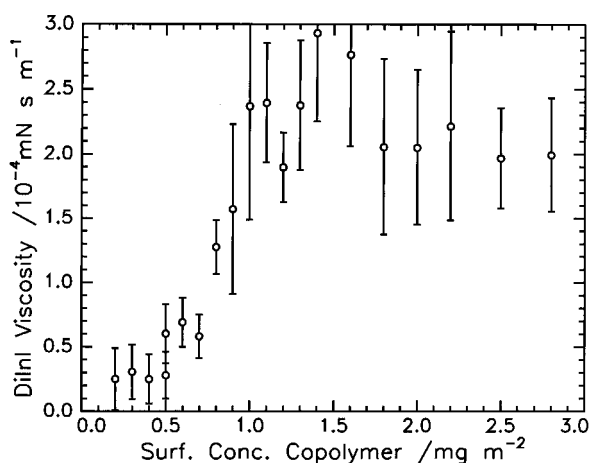


Fig. 9 Dilatational viscosity (ε') as a function of surface concentration (Γ_s).

scattering data scales as $\Gamma_s^{3.5}$ and a maximum in the variation of ϵ_0 with Γ_s is not predicted. Secondly, there is considerable difference in the dilatational modulus values when the surface concentration exceeds $\sim 1.2 \text{ mg m}^{-2}$. This difference may be due to the different time and length scales involved in each experiment. The light scattering experiments are on time scales of $\sim (1/\omega_0)$ and involve microscopic displacements of the spread film. Classical values of ϵ_0 involve macroscopic compression of the film and finite times during which time the film may rearrange to a configuration which differs from that sampled by the light scattering.

We note that the surface tensions from surface light scattering and surface pressure data ‘cross’ at $\Gamma_s \approx 1.5 \text{ mg m}^{-2}$, thereafter the γ_0 values from light scattering being the larger. The dilatational viscosity has a maximum at $\Gamma_s \approx 1.5 \text{ mg m}^{-2}$; eqn. (10) predicts that it should continue to increase with σ_0 , which conforms to the view that the dilatational viscosity arises from the permeation of the solvent through the brush like layer. Therefore, the rather distinctive and abrupt change in ϵ_0 and ϵ' over $1.0 \leq \Gamma_s/\text{mg m}^{-2} \leq 1.5$ suggests a change in the arrangement of the VPQ units at the air/water interface. Opposing this view are the neutron reflectometry values of the thickness of the VPQ layer,³⁶ which are shown in Fig. 10 as a function of surface concentration. Although the region occupied by the VPQ blocks increases in thickness as Γ_s increases, this appears to be continuous rather than taking place over a very small Γ_s range as suggested by the change in ϵ_0 and ϵ' . Furthermore, the number density of VPQ units in this layer is rather constant at $8.2 \pm 1 \times 10^{-4} \text{ m}^{-3}$ over the concentration range $1.0\text{--}3.0 \text{ mg m}^{-2}$. Another factor that may have some bearing here is the polyelectrolyte nature of the VPQ blocks. This type of block was deliberately selected because it should be strongly associated with the aqueous subphase and the high degree of dissociation of the quaternised vinyl pyridine residues leads to strong polyelectrolyte behaviour and there should be stretching to reduce Coulombic interactions between adjacent units. Complicating factors include counter-ion condensation³⁷ onto the polyelectrolyte block, which may thus not be as extended as would be anticipated for complete dissociation of the VPQ units.

Visco-elastic properties

Apart from the dispersion behaviour (*vide infra*), visco-elastic behaviour is evident if there is a capillary wave frequency dependence of the surface moduli. At resonance, as we remarked earlier the real frequencies of the two modes are equal, hence we can use the observed capillary wave frequencies to interpret the dilatational moduli as well as the surface tension. The dependence of capillary wave frequency and damping on wavenumber (q) at a block copolymer surface concentration of 0.8 mg m^{-2} is shown in Fig. 11, which includes lines for the same quantities for the

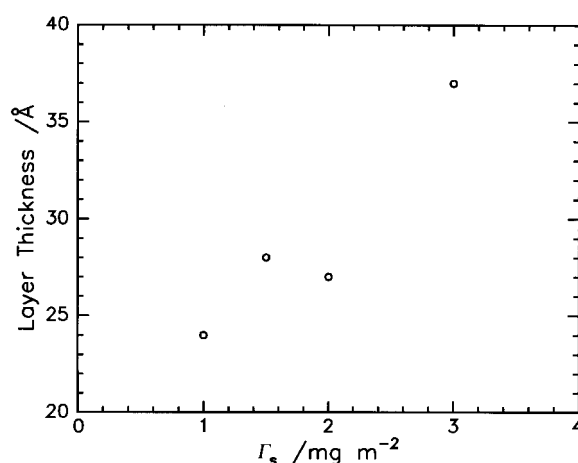


Fig. 10 Thickness (from neutron reflectometry) of the near surface region occupied by VPQ units as a function of surface concentration of PMMA-VPQ copolymer.

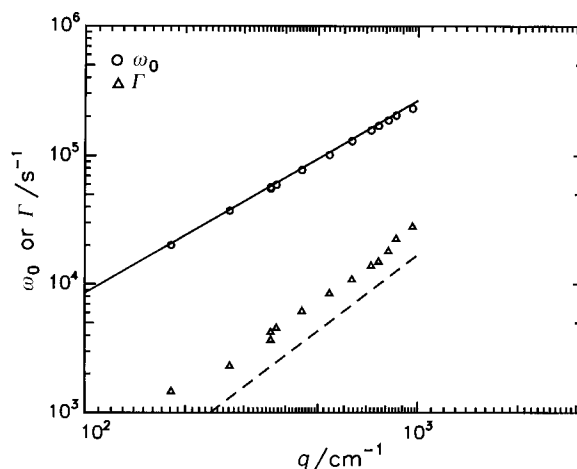


Fig. 11 Wavenumber dependence of frequency and damping for a PMMA-VPQ spread film at $\Gamma_s = 0.8 \text{ mg m}^{-2}$. The lines are the calculated frequencies and dampings for a clean water surface.

clean water surface calculated from the first-order approximations to ω_0 and Γ in eqn. (13). As q increases, the frequency becomes slightly smaller than the values for clean water. The observed damping, however, is always larger than that of the clean water surface and there appears to be an increasing divergence at higher q values.

The frequency dependences of the surface tension, dilatational modulus and dilatational viscosity (the latter as a loss modulus, see below) at the 'resonance concentration' of 0.8 mg m^{-2} are shown in Fig. 12. Since spread films of PMMA do not exhibit any frequency dependence of the moduli (in the range accessible to surface light scattering), then the presence of the VPQ block is solely responsible for the observed behaviour. A simple model frequently invoked to describe this visco-elastic behaviour is that of a Maxwell fluid. The basis of this model is the concept that the spread surface film is subjected to oscillatory stress and strain by the capillary waves. The stress and strain are connected *via* the complex modulus

$$G^*(\omega) = G'(\omega) + iG''(\omega)$$

where $G'(\omega)$ is the storage modulus and is equivalent to γ_0 or ε_0 and $G''(\omega)$ is the loss modulus equivalent to $\omega_0 \varepsilon'(\omega)$ here. For a Maxwell fluid,⁵

$$G'(\omega) = G_{\text{eq}} + S \left(\frac{\omega^2 \tau^2}{1 + \omega^2 \tau^2} \right) \quad (15)$$

$$G''(\omega) = S \left(\frac{\omega \tau}{1 + \omega^2 \tau^2} \right) \quad (16)$$

where G_{eq} is the zero frequency value of the modulus, S the strength of the relaxation process which has a relaxation time τ . The lines on each of the plots are the best non-linear least squares fit to the data. From these fits, the relaxation time is approximately the same for both transverse and dilatational modes at $ca. 3 \pm 1 \mu\text{s}$ although there is a considerable error for the relaxation time extracted from the loss modulus values. The equilibrium surface tension and dilatational modulus are 71 and 10 mN m^{-1} , the value for the surface tension being consistent with the surface pressure recorded at this resonance concentration (*i.e.*, $\sim 0 \pm 2 \text{ mN m}^{-1}$).

Eqns. (15) and (16) can be combined to provide an expression for the relaxation time that enables the surface concentration dependence to be assessed:

$$\tau = \frac{G'(\omega) - G_{\text{eq}}}{\omega_0 G''(\omega)} \quad (17)$$

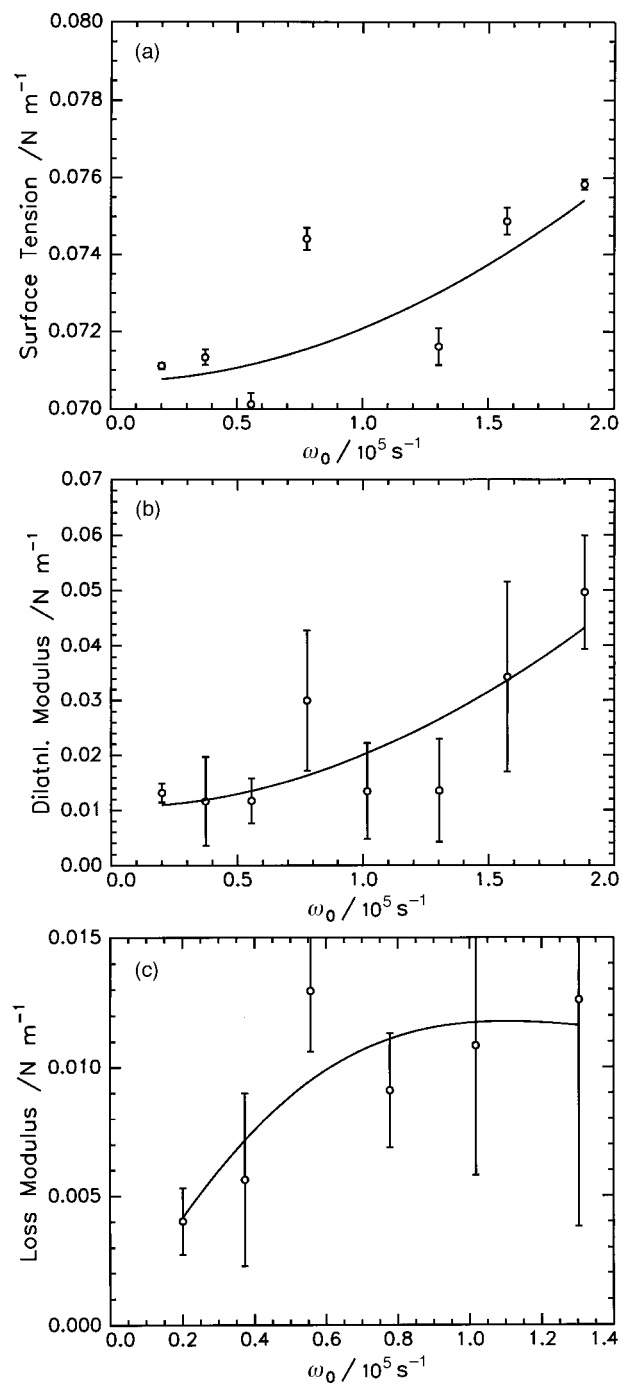


Fig. 12 Frequency dependence of surface tension (a), dilatational modulus (b) and loss modulus [$\equiv \omega_0 \varepsilon''(\omega)$] (c) for a spread film concentration of 0.8 mg m^{-2} . The lines are non-linear least squares fits of a Maxwell fluid model to the data.

where

$$G'(\omega) - G_{\text{eq}} = \varepsilon_0 - \varepsilon_{\text{ST}}$$

and

$$\omega_0 G''(\omega) = \omega_0^2 \varepsilon'$$

If the relaxation process is well described by a Maxwell fluid model, which presumes a single exponential relaxation process, then a semi-log plot of the relaxation times as a function of surface concentration should be linear. Fig. 13 shows such a semi-logarithmic plot and a linear dependence is evident in the region of surface concentration where the classical dilatational modulus is less than the light scattering determined value. There are two comments to make regarding this plot. First, because we have had to use the capillary wave frequency (rather than the unobservable dilatational wave frequency) in eqn. (17), the relaxation times are 'apparent' values; however the general dependence on the surface concentration (*i.e.*, an exponential dependence) will still be valid. Secondly, the relaxation time decreases as the surface concentration increases rather than increasing or remaining constant as might have been expected from the small change in the concentration of VPQ units as the surface concentration increases. For the VPQ layer thicknesses determined, it is evident that the VPQ does not have the rigid rod configuration expected for a fully dissociated polyelectrolyte. We speculate that increased counter-ion condensation takes place as the surface concentration increases and the initially rod-like configuration of the VPQ becomes more of a flexible coil at higher concentrations. The longer relaxation times are associated with the rod-like configuration, the shorter times with the random coil. Unfortunately for surface concentrations less than 1 mg m^{-2} , the VPQ is far too dilute to be observable by neutron reflectometry.

Dispersion behaviour

The values of the surface visco-elastic parameters obtained are dependent on the form of the dispersion equation used in the interpretation of the light scattering data. Consequently the omission of some parameters (γ' , λ_0 and λ') may make the accuracy of those parameters that are determined questionable. The various models may be distinguishable from comparing the dispersion behaviour with that observed experimentally, *i.e.*, plotting the damping as a function of the capillary wave frequency. The evaluation of these two parameters does not depend on a model and thus is not subject to any uncertainties. Earnshaw and McLaughlin^{38,39} have discussed the influence of ε' and γ' on dispersion behaviour and have demonstrated the conditions under which mode mixing is obtained. The dispersion plot for the data obtained at the surface concentration of 0.8 mg m^{-2} is shown in Fig. 14 as normalised damping and normalised frequency, *i.e.*, $\Gamma/(2\eta q^3/\rho)$

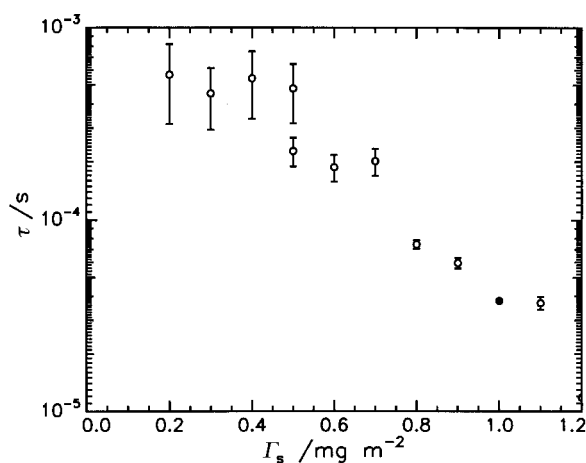


Fig. 13 Apparent relaxation time calculated from eqn. (17), using dilatational moduli and viscosities and capillary wave frequencies, plotted in semi-logarithmic form as a function of the surface concentration of the block copolymer.

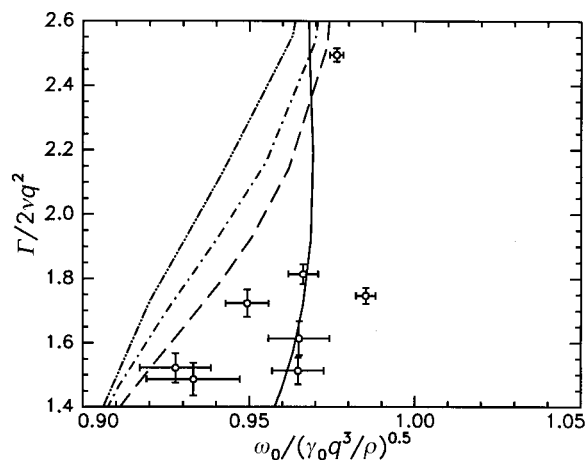


Fig. 14 Dispersion plot of normalised damping as a function of normalised frequency for the PMMA-VPQ copolymer spread film at a surface concentration of 0.8 mg m^{-2} compared with the predicted behaviour from the two forms of the dispersion equation. Solid line from eqn. (4) with $\gamma' = 0$ and average values of γ_0 , ϵ_0 and ϵ' over the range of q explored. The dashed lines have values of λ' increasing in magnitude from left to right of -2×10^{-7} , -4×10^{-7} and $-6 \times 10^{-7} \text{ mN s m}^{-1}$.

and $\omega_0/(\gamma_0 q^3/\rho)^{1/2}$. Included in Fig. 14 are dispersion behaviours predicted for each of the dispersion eqns. [(4) and (12)] using average values of γ_0 , ϵ_0 and ϵ' over the q range explored. The dashed and dashed-dot lines show the behaviour anticipated if the coupling factor, λ , was playing a role. Since we ascertained earlier that λ_0 had little influence on frequency and damping, this has been fixed at $10^{-4} \text{ mN m}^{-1}$ and λ' varied from 2×10^{-7} to $6 \times 10^{-7} \text{ mN s m}^{-1}$. The classical dispersion equation [eqn. (4)] appears to be the better description of the experimental data, the disagreement at higher q values being due to the changing values of the surface visco-elastic parameters at higher q values in the experimental data whereas average values have been used to calculate the dispersion behaviour.

Conclusions

The surface visco-elastic behaviour of a linear diblock copolymer, in which one of the blocks is a polyelectrolyte, at the air/water interface has been examined using surface quasi-elastic light scattering. These data were analysed with a small modification of the dispersion equation suggested by a recent re-analysis of the influence of capillary waves on a polymer brush at fluid interfaces. Because the layer of the polyelectrolyte-containing block had only modest dimensions, the incorporation of a coupling parameter suggested by the re-analysis was not required. Dilatational moduli obtained by light scattering exhibited a maximum as the surface concentration of the block copolymer increased and, at the same surface concentration where the maximum was observed, the dilatational viscosity attained a plateau value. The dilatational moduli from surface pressure data are initially smaller than those obtained by light scattering but at higher surface concentrations they greatly exceed the light scattering dilatational moduli. The finite compression of the film and the relatively long time required for this compression (compared to the capillary wave perturbations) were cited as possible causes for this discrepancy. However, the observation of a maximum in the light scattering values of the dilatational modulus is not predicted by the theoretical analysis for electrically neutral polymers. Capillary wave frequency dependent values of surface tension, dilatational modulus and dilatational viscosity, all obtained at a surface concentration where resonance between dilatational and capillary modes occurs, can be adequately represented by using a Maxwell fluid model with a relaxation time of *ca.* $3 \mu\text{s}$ for the spread polymer film. The dependence of the 'apparent' relaxation time of the dilatational mode appears to conform to a single exponential relaxation consistent with a Maxwell fluid model. A noteworthy

feature was the decrease in relaxation time as the surface concentration increased and it has been speculated that this may be due to counter-ion condensation on the polyelectrolyte block leading to the block having a more coil like character.

References

- 1 J. Lucassen, *Trans. Faraday Soc.*, 1968, **64**, 2221.
- 2 V. G. Levich, *Physicochemical Hydrodynamics*, Prentice-Hall, Englewood Cliffs, NJ, 1962.
- 3 A. B. Pippard, *The Physics of Vibration, Omnibus Edition*, Cambridge University Press, Cambridge, 1989.
- 4 A. B. Pippard, *Response and Stability*, Cambridge University Press, Cambridge, 1985.
- 5 J. D. Ferry, *Visco-Elastic Properties of Polymers*, John Wiley, New York, 1980.
- 6 F. C. Goodrich, *Proc. R. Soc. London A*, 1981, **374**, 341.
- 7 E. H. Lucassen-Reynders and J. Lucassen, *Adv. Colloid Interface Sci.*, 1969, **2**, 347.
- 8 M. Hennenberg, X.-L. Chu, A. Sanfeld and M. G. Velarde, *J. Colloid Interface Sci.*, 1992, **150**, 7.
- 9 X.-L. Chu and M. G. Velarde, *PCH PhysicoChem. Hydrodyn.*, 1988, **10**, 727.
- 10 M. G. Velarde, *Philos. Trans. R. Soc. London Ser. A*, 1998, **356**, 829.
- 11 J. C. Earnshaw and E. McCoo, *Langmuir*, 1995, **11**, 1087.
- 12 J. L. Harden and H. Pleiner, *Phys. Rev. E*, 1994, **49**, 1411.
- 13 F. C. Goodrich, *J. Phys. Chem.*, 1962, **66**, 1858.
- 14 S. K. Peace, R. W. Richards and N. Williams, *Langmuir*, 1998, **14**, 667.
- 15 D. M. A. Buzza, J. L. Jones, T. C. B. McLeish and R. W. Richards, *J. Chem. Phys.*, 1998, **109**, 5008.
- 16 R. H. Katyl and K. U. Ingard, *Phys. Rev. Lett.*, 1968, **20**, 248.
- 17 C. Booth, R. W. Richards, M. R. Taylor and G. E. Yu, *J. Phys. Chem. B*, 1998, **102**, 2001.
- 18 J. F. Crilly and J. C. Earnshaw, *Biophys. J.*, 1983, **41**, 197.
- 19 J. C. Earnshaw and P. J. Winch, *Thin Solid Films*, 1988, **159**, 159.
- 20 J. C. Earnshaw and D. J. Sharpe, *J. Chem. Soc., Faraday Trans.*, 1996, **92**, 611.
- 21 R. W. Richards and M. R. Taylor, *J. Chem. Soc., Faraday Trans.*, 1996, **92**, 601.
- 22 R. W. Richards, B. R. Rochford and M. R. Taylor, *Macromolecules*, 1996, **29**, 1980.
- 23 R. W. Richards and M. R. Taylor, *Macromolecules*, 1997, **30**, 3892.
- 24 F. E. Runge, H. Yu and D. Woermann, *Ber. Bunsen-Ges. Phys. Chem.*, 1994, **98**, 1046.
- 25 K. Sakai and K. Takagi, *Langmuir*, 1994, **10**, 257.
- 26 D. Sharpe and J. Eastoe, *Langmuir*, 1995, **11**, 4636.
- 27 D. Sharpe and J. Eastoe, *Langmuir*, 1996, **12**, 2303.
- 28 M. van den Tempel and E. H. Lucassen-Reynders, *Adv. Colloid Interface Sci.*, 1983, **18**, 281.
- 29 S. K. Peace, R. W. Richards, M. R. Taylor, J. R. P. Webster and N. Williams, *Macromolecules*, 1998, **31**, 1261.
- 30 P. G. de Gennes, *Macromolecules*, 1980, **13**, 1069.
- 31 J. Lyklema, *Fundamentals of Interface and Colloid Science*, Academic Press, London, 1991.
- 32 D. Langevin, in *Light Scattering by Liquid Surfaces and Complementary Techniques*, ed. D. Langevin, Dekker, New York, 1992.
- 33 R. W. Richards, B. R. Rochford and M. R. Taylor, *Macromolecules*, 1996, **29**, 1980.
- 34 J. C. Earnshaw, R. C. McGivern, A. C. McLaughlin and P. J. Winch, *Langmuir*, 1990, **6**, 649.
- 35 J. C. Earnshaw, R. C. McGivern and P. J. Winch, *J. Phys.*, 1988, **49**, 1271.
- 36 A. S. Brown and R. W. Richards, unpublished data.
- 37 H. Dautzenberg, W. Jaeger, W. Kotz, B. Philipp, C. Seidel and D. Stscherbina, *Polyelectrolytes Formation, Characterization and Application*, Hanser, Munich, 1994.
- 38 J. C. Earnshaw and A. C. McLaughlin, *Proc. R. Soc. London A*, 1991, **433**, 663.
- 39 J. C. Earnshaw and A. C. McLaughlin, *Proc. R. Soc. London A*, 1993, **440**, 519.

Paper 8/09091B